

Charge-order-induced sharp Raman peak in $\text{Sr}_{14}\text{Cu}_{24}\text{O}_{41}$

K.P. Schmidt¹, C. Knetter¹, M. Grüninger², and G.S. Uhrig¹

¹*Institut für Theoretische Physik, Universität zu Köln, Zùlpicher Straße 77, D-50937 Köln, Germany*

²*II. Physikalisches Institut, Universität zu Köln, Zùlpicher Straße 77, D-50937 Köln, Germany*

(revised version: February 3, 2003)

In the two-leg $S=1/2$ ladders of $\text{Sr}_{14}\text{Cu}_{24}\text{O}_{41}$ a modulation of the exchange coupling arises from the charge order within the other structural element, the CuO_2 chains. In general, breaking translational invariance by modulation causes gaps within the dispersion of elementary excitations. We show that the gap induced by the charge order can drastically change the magnetic Raman spectrum leading to the sharp peak observed in $\text{Sr}_{14}\text{Cu}_{24}\text{O}_{41}$. This sharp Raman line gives insight in the charge-order periodicity and hence in the distribution of carriers. The much broader spectrum of $\text{La}_6\text{Ca}_8\text{Cu}_{24}\text{O}_{41}$ reflects the response of an undoped ladder in the absence of charge order.

PACS numbers: 75.40.Gb, 75.10.Jm, 74.25.Ha, 75.50.Ee

Understanding the complex interplay of spin and charge degrees of freedom in doped quantum-spin systems is a key issue in condensed matter physics. This interplay governs in particular the physics of the planar high- T_c superconducting cuprates. In the telephone-number compounds $\text{A}_{14}\text{Cu}_{24}\text{O}_{41}$ it gives rise to a variety of interesting ground states. In $\text{La}_6\text{Ca}_8\text{Cu}_{24}\text{O}_{41}$ the ladders form an insulating spin liquid [1]. $\text{Sr}_{14-x}\text{Ca}_x\text{Cu}_{24}\text{O}_{41}$ becomes superconducting under external pressure for $x \gtrsim 11.5$ [2,3] whereas an insulating charge-ordered state is favored for $x \lesssim 5$ [1,4–9], although the average copper valence does not depend on x . The different properties are usually attributed to the different distribution of charges between the two subsystems [10,11], Cu_2O_3 two-leg ladders and CuO_2 chains [12]. But the interesting physics linked to the differing periodicity of ladders and chains [13] is usually neglected.

Raman scattering offers a powerful tool to examine the spectral density of magnetic excitations and thus provides important information on the kinetics and on the interactions of the elementary excitations. In the undoped spin liquid $\text{La}_6\text{Ca}_8\text{Cu}_{24}\text{O}_{41}$, the ladders show a very broad two-triplet Raman line with slightly different peak positions for leg-leg and rung-rung polarization [14]. This agrees very well with theoretical results [15]. A very different line shape, however, is found in charge-ordered $\text{Sr}_{14}\text{Cu}_{24}\text{O}_{41}$, which shows a peculiar sharp peak that is observed at the same frequency in both polarizations [14,16]. This sharp response poses a challenge to the understanding of the cuprate ladders and offers the opportunity to study the interplay of spin and charge degrees of freedom in this fascinating system.

The sharpness of the Raman peak in $\text{Sr}_{14}\text{Cu}_{24}\text{O}_{41}$ is in strong contrast to the very broad two-magnon Raman line observed in the undoped two-dimensional (2D) high- T_c cuprates, which is still the subject of controversial discussions. Gozar *et al.* [16] argued that the observation of a very sharp two-triplet Raman line in a one-dimensional

(1D) spin liquid suggests that the large width found in 2D cannot be attributed to quantum fluctuations.

Here, we challenge this point of view by providing a clear explanation for the Raman data of $\text{Sr}_{14}\text{Cu}_{24}\text{O}_{41}$. We propose that the charge-order superstructure gives rise to a modulation of the exchange coupling along the ladders. The concomitant backfolding of the dispersion of the elementary triplet opens gaps at the crossing points. This in turn can have a drastic effect on the Raman line shape, which we calculate using continuous unitary transformations (CUTs) [17,15]. The high resolution accessible by the CUT approach is decisive to account for the very narrow peak we are aiming at. Our results with and without charge order excellently describe the Raman data of $\text{Sr}_{14}\text{Cu}_{24}\text{O}_{41}$ and $\text{La}_6\text{Ca}_8\text{Cu}_{24}\text{O}_{41}$, respectively.

For zero hole doping, the minimal model for the magnetic properties of the $S = 1/2$ two-leg ladders in $\text{A}_{14}\text{Cu}_{24}\text{O}_{41}$ is an antiferromagnetic Heisenberg Hamiltonian plus a cyclic four-spin exchange term H_{cyc} [18–20]

$$H = J_{\perp} \sum_i \mathbf{S}_{i,1} \mathbf{S}_{i,2} + J_{\parallel} \sum_{i,\tau} \mathbf{S}_{i,\tau} \mathbf{S}_{i+1,\tau} + H_{\text{cyc}} \quad (1a)$$

$$H_{\text{cyc}} = J_{\text{cyc}} \sum_i K_{(i,1),(i,2),(i+1,2),(i+1,1)} \quad (1b)$$

$$K_{1234} = (\mathbf{S}_1 \mathbf{S}_2)(\mathbf{S}_3 \mathbf{S}_4) + (\mathbf{S}_1 \mathbf{S}_4)(\mathbf{S}_2 \mathbf{S}_3) - (\mathbf{S}_1 \mathbf{S}_3)(\mathbf{S}_2 \mathbf{S}_4) \quad (1c)$$

where i denotes the rungs and $\tau \in \{1, 2\}$ the legs. The exchange couplings along the rungs and along the legs are denoted by J_{\perp} and J_{\parallel} , resp.. There is also another way to include the leading four-spin exchange term by cyclic permutations [21,20] which differs in certain two-spin terms from Eq. (1) [21]. Both Hamiltonians are identical except for couplings along the diagonals if J_{\perp} and J_{\parallel} are suitably redefined [22]. Here, we use Hamiltonian (1) since it is established that the four-spin terms are the significant ones [24]. The exchange parameters determined in Ref. [20] for $\text{La}_{5.2}\text{Ca}_{8.8}\text{Cu}_{24}\text{O}_{41}$ correspond in our nota-

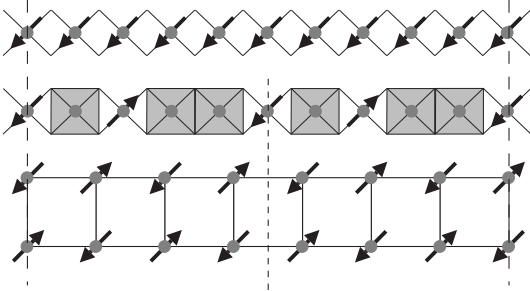


FIG. 1. Scheme [23] of the superstructure along the chains and the ladders (c axis). 10 chain units (top row) match 7 ladder units (bottom row) inducing a modulation in the ladders with wave vector $Q_S = c_{\text{ladder}}/c_{\text{chain}} = 10/7 = 3/7 + 1$ (in r.l.u. of the ladder) [13]. In $\text{Sr}_{14}\text{Cu}_{24}\text{O}_{41}$ the charge order (CO) implies an additional superstructure with $Q_{\text{CO}} = 2/10$ (in r.l.u. of the *chain*) [4–7], corresponding to a periodicity of $5 \cdot c_{\text{chain}}$. It is visualized (middle row) as two units of “spin-hole-spin-hole-hole” per 7 rungs (grey squares denote the six holes per f.u.). This superstructure induces an additional modulation in the ladder with $Q_{\text{CO}} = c_{\text{ladder}}/(5 \cdot c_{\text{chain}}) = 2/7$ (in r.l.u. of the ladder).

tion [22] to $J_{\parallel}/J_{\perp} = 1.22 \pm 0.05$, $J_{\text{cyc}}/J_{\perp} = 0.21 \pm 0.03$ and $J_{\perp} = 1150 \pm 100 \text{ cm}^{-1}$. Using the average values, we find within 5% the same values for the spin gap and for the two-triplet bound-state energies as in Ref. [20].

The exchange coupling in the CuO_2 chains is much weaker than in the ladders since it is mediated via Cu-O-Cu bonds with an angle close to 90° . Thus the chains do not contribute directly to the Raman line at $\approx 3000 \text{ cm}^{-1}$. But the presence of the chains gives rise to 7 inequivalent ladder rungs per formula unit (f.u.) and thereby induces a modulation in the ladders (see Fig. 1). This modulation is characterized by the wave vector $Q_S = 10/7 = 3/7 + 1$ in reciprocal lattice units (r.l.u.) of the ladder. In the magnetic subsystem of the spins on the Cu sites of the ladder, wave vectors are only meaningful modulo unity so that $Q_S = 10/7$ and $Q_S = 3/7$ are equivalent. The additional modulation induced by the charge ordering on the chains below $T_{\text{CO}} \approx 200 \text{ K}$ has the wave vector $Q_{\text{CO}} = 2/7$ [4–7], see Fig. 1.

Now we estimate the amplitude of the exchange modulation with Q_S . The Cu-O distances within the ladder are hardly affected by the modulation; the main effect is a shift of the O ions perpendicular to the Cu-O-Cu bonds [13]. Hence the electronic hopping elements t_{pd} can safely be considered constant. The exchange couplings are modified by the induced variation of the charge-transfer energy Δ_{ct} , i.e. the variation of the energy difference between holes on Cu and on O. We computed the variation of Δ_{ct} in a point-charge model with stoichiometric valencies except for the chain oxygen with $q = -1.7e$ to account for the holes [10,11]. The calculation uses Ewald sums so that the results pertain to the infinite system. The relative changes $\Delta J/J$ are estimated in leading order [24]. Assuming structurally un-

modulated chains and ladders, we find a negligible effect of the chains on the exchange couplings of the ladder of $|\Delta J/J| \lesssim 10^{-6}$. However, the *modulated* positions at 300 K [13] yield

$$J_{\parallel,i} = J_{\parallel} [1 + 0.05 \cos(2\pi \frac{3}{7}(i + \frac{1}{2}))] \quad (2a)$$

$$J_{\perp,i} = J_{\perp} [1 - 0.10 \sin(2\pi \frac{3}{7}i) + 0.05 \cos(2\pi \frac{6}{7}(i+3))] \quad (2b)$$

with phase accuracy $|\Delta i| \lesssim 0.1$ [23] where i counts the leg- or the rung-bonds. The term with $2Q_S = 6/7$ denotes the second harmonic; overtones with amplitude $\lesssim 1\%$ are omitted. The amplitudes in Eq. (2) show that the induced modulation of the couplings is indeed sizeable.

We expect that the effects of the charge order occurring below $T_{\text{CO}} \approx 200 \text{ K}$ are of similar size. Without detailed information on the structure at $T \ll T_{\text{CO}}$, only an estimate is possible. We assume a charge modulation on the chain oxygen of $\Delta q(j) = -0.2e \cos(2\pi \frac{2}{10}(j + \frac{1}{2}))$, where j counts the chain O sites, and the periodicity $5c_{\text{chain}}$ and the phase are established experimentally [4–7] (cf. middle row of Fig. 1). This yields an additional modulation

$$\Delta J_{\parallel,i} = 0.16 J_{\parallel} \cos(2\pi \frac{2}{7}i), \quad (3)$$

with phase accuracy of $|\Delta i| \lesssim 0.1$ [23]. Thus the modulation induced by the charge order with $Q_{\text{CO}} = 2/7$ (in r.l.u. of the ladder) is indeed significant.

Now, we investigate the effects of modulations on magnetic Raman scattering which probes the excitations with zero momentum and zero spin. At $T=0$ the Raman response $I(\omega)$ is given by the retarded resolvent

$$I(\omega) = \frac{-1}{\pi} \lim_{\delta \rightarrow 0^+} \text{Im} \left\langle 0 \left| R^\dagger \frac{1}{\omega - H + E_0 + i\delta} R \right| 0 \right\rangle. \quad (4)$$

The observables R^{rung} (R^{leg}) for magnetic light scattering in rung-rung (leg-leg) polarization are given in Ref. [15]. We focus on the dominant two-triplet contribution. A CUT is employed to map the Hamiltonian H to an effective Hamiltonian H_{eff} which conserves the number of rung-triplets [17,25,15]. The ground state of H_{eff} is the rung-triplet vacuum. The observable R in $I(\omega)$ is mapped by the same unitary transformation to an effective observable R_{eff} .

The CUT is implemented perturbatively in J_{\parallel}/J_{\perp} . We compute H_{eff} and R_{eff} to order $n \geq 10$. A calculation in order n accounts for hopping and interaction processes extending over a distance of n rungs. The resulting plain series are represented in terms of the variable $1 - \Delta/(J_{\parallel} + J_{\perp})$ [26]. Then standard Padé approximants [27] yield reliable results up to $J_{\parallel}/J_{\perp} \approx 1 - 1.5$ depending on the value of J_{cyc}/J_{\perp} . Consistency checks were carried out by extrapolating the involved quantities before and after Fourier transforms. In case of inconclusive approximants the bare truncated series are used. We estimate the overall accuracy to be $\approx 5\%$. The Raman line shape is finally calculated as continued fraction by tridiagonalization of the effective two-triplet Hamiltonian in a

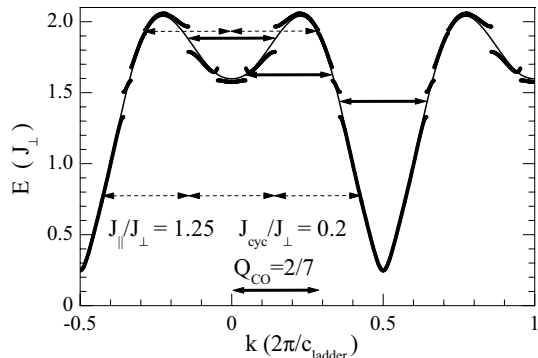


FIG. 2. Dispersion of the elementary triplets with (thick line) and without (thin line) a modulation of $\alpha_{2/7}=0.15$ (cf. Eq. 5) with $Q_{CO} = 2/7$ (arrows). Some higher-order contributions are denoted by dashed arrows.

mixed representation using the total momentum and the real-space distance. So the total momentum is sharply defined. No finite-size effects appear. This ensures a particularly high resolution in momentum and in energy necessary to account for a very sharp feature.

The modulation is included on the level of the effective model, i.e. *after* the CUT. This is no serious caveat since a microscopic calculation is not available. The leading-order effect of J_{\parallel} is to enable the elementary triplets to hop from rung to rung by a nearest-neighbor hopping element $t_1 \propto J_{\parallel}$ and to induce a nearest-neighbor interaction $w_1 \propto J_{\parallel}$. So the most straightforward way to account for the modulation of J_{\parallel} as given in Eqs. (2a) and (3) is to modulate t_1 and w_1 ,

$$t_1 \propto w_1 \propto J_{\parallel} \cdot \left[1 + \sum_{Q=2/7, 3/7, 6/7} \alpha_Q \cos(2\pi Qi) \right]. \quad (5)$$

Since we focus on the effect of the charge order (Eq. 3), the modulation of J_{\perp} as given in Eq. (2b) is neglected.

We use the parameters fixed for $\text{La}_{5.2}\text{Ca}_{8.8}\text{Cu}_{24}\text{O}_{41}$ in Refs. [20,22], $J_{\parallel}/J_{\perp}=1.25$ and $J_{\text{cyc}}/J_{\perp}=0.2$. Fig. 2 shows the dispersion with and without a 15% modulation with wave vector Q_{CO} , i.e. $\alpha_{2/7}=0.15$ in Eq. (5). Clearly, sizeable gaps open wherever Q_{CO} links equal energies $\omega(k) = \omega(k + Q_{CO})$ of the unmodulated ladder. Smaller gaps open for higher-order processes, e.g. for $\omega(k) = \omega(k + 2Q_{CO})$. Thus the energies at which gaps open depend decisively on the wave vector of the modulation.

The Raman response of an undoped and unmodulated ladder is very broad (bottom panel of Fig. 3 and Ref. [15]), in good agreement with data of $\text{La}_6\text{Ca}_8\text{Cu}_{24}\text{O}_{41}$ [14] (middle panel of Fig. 3). The excellent description of the peak position obtained for the parameter set of Ref. [20] given above corroborates these parameters. What is the effect of a modulation on the Raman line shape? The occurrence of gaps implies prominent peaks (van Hove singularities) in the density of states (DOS) and hence in the Raman line shape. Since Raman scattering measures

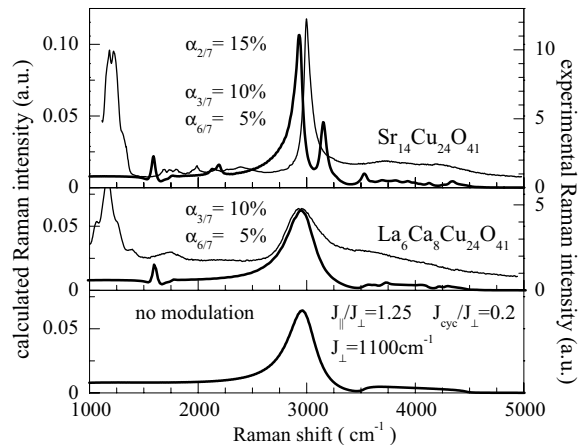


FIG. 3. Thick lines: Raman line shapes in leg-leg polarization for $J_{\parallel}/J_{\perp} = 1.25$, $J_{\text{cyc}}/J_{\perp} = 0.2$ and $J_{\perp}=1100 \text{ cm}^{-1}$ [20,22] without modulation (bottom), with the structural modulation $Q_S=3/7$ and $6/7$ appropriate for $\text{La}_6\text{Ca}_8\text{Cu}_{24}\text{O}_{41}$ (middle) and with the additional charge-order modulation of $\text{Sr}_{14}\text{Cu}_{24}\text{O}_{41}$ (top). Thin lines: Raman data from Ref. [14], $T=20\text{K}$. A modulation-induced gap in the dispersion at ω_g (see Fig. 2) causes a Raman feature at $2\omega_g$. Additional features arise due to backfolding, e.g. the small peak at 2200 cm^{-1} corresponds to the $S=0$ two-triplet bound state at $k=2/7$ [25].

excitations with total momentum $k_{\text{tot}}=0$, the two-triplet response reflects the excitation of two triplets with momenta $k_2 = -k_1$ and energies $\omega(k_1) = \omega(k_2)$. A gap at ω_g thus causes a corresponding feature in the Raman line at $2\omega_g$. For the structural wave vectors $Q_S=3/7$ and $6/7$ these effects are rather small (middle panel of Fig. 3). But a drastic change of the line shape appears if (and only if) $2\omega_g$ coincides with the broad peak of the unmodulated ladder, since then the opening of the gap implies a redistribution of a large part of the spectral weight. For the relevant exchange couplings we find that $2 \cdot \omega(\pi/c_{\text{ladder}} \pm Q_{CO}/2) \approx 2.8J_{\perp} \approx 3100 \text{ cm}^{-1}$ is slightly above the Raman peak of the unmodulated ladder. Hence the charge-order modulation piles up a large part of the high-frequency weight on top of the peak, giving rise to a very sharp feature which agrees very well with the data of $\text{Sr}_{14}\text{Cu}_{24}\text{O}_{41}$ [14,16] (top panel of Fig. 3). Since both the exchange constants in $\text{Sr}_{14}\text{Cu}_{24}\text{O}_{41}$ and the calculations are accurate within a few percent, only a semi-quantitative analysis is possible which shows the principal mechanism. The remaining uncertainties may imply that also a smaller value of $\alpha_{2/7}$ is sufficient to produce the sharp feature.

The good agreement between the experimental data and the theoretical result, based on the independently determined couplings [20,22] and the wave vector of the charge order, corroborates our interpretation. Another argument stems from the polarization dependence. For $J_{\text{cyc}} > 0$, the peak positions for leg-leg and rung-rung polarization should be different [15]. This is indeed

the case in $\text{La}_6\text{Ca}_8\text{Cu}_{24}\text{O}_{41}$ [14], but the sharp peak in $\text{Sr}_{14}\text{Cu}_{24}\text{O}_{41}$ is found at $\approx 3000 \text{ cm}^{-1}$ in *both* polarizations [14,16]. In the scenario of the modulation-induced gaps the peak position is determined by the position and the size of the gap, since the peak is primarily a DOS effect. Hence the coincidence of the peak positions in both polarizations despite $J_{\text{cyc}} > 0$ supports our scenario. Moreover, also the spectra of $\text{Sr}_{14}\text{Cu}_{24}\text{O}_{41}$ at elevated temperatures are explained. The charge order melts at $T_{\text{CO}} \approx 200 \text{ K}$. Indeed, the very sharp Raman line is observed only below T_{CO} [14]. For $T \geq T_{\text{CO}}$, the peak positions are *different* for the two polarizations [14], which is expected for $J_{\text{cyc}} \approx 0.2J_{\perp}$ at $\alpha_{2/7} = 0$.

An alternative explanation of the sharp peak in terms of bound states is unlikely. There is no bound state within the broad Raman continuum of the undistorted, undoped ladder [15]. But how about finite doping? At 300 K, about 90 % of the doped carriers reside in the chains [10]. At low temperatures the distribution of holes is not yet settled experimentally. Theoretically, the Madelung potentials indicate that all the holes reside in the chains [11]. This is corroborated by the observation of the periodicity $5c_{\text{chain}}$ [4–7] for the charge order in the chains. In a 1D fermionic system it is natural to view the charge order as an effect of the $2k_{\text{F}}$ instability. So we are led to conclude that $2k_{\text{F}} = 2/10$ (in r.l.u. of the chain), which implies that there are $n_{\downarrow} + n_{\uparrow} = 4/10$ electrons per site or 6 holes per f.u.. This further supports our assumption that at $T \approx 0$ all holes reside on the chains.

A finite hole concentration on the ladders cannot be ruled out completely. These charges would be pinned in a commensurate charge-density wave (CDW) at low temperatures by the electrostatic potential of the charge order on the chains. Clearly, such a CDW would also induce strong modulations. But it remains unclear where the peculiar periodicity stems from if $2k_{\text{F}} \neq 2/10$.

A small amount of impurity holes cannot explain the sharp Raman peak. Below T_{CO} , $\text{Sr}_{14}\text{Cu}_{24}\text{O}_{41}$ is insulating, i.e. all charge carriers are localized. The local charge degrees of freedom may couple to the magnetic ones, but due to the local character the whole Brillouin zone would be involved implying a *broad* energy distribution, at odds with experiment [14,16].

Our results clearly call for several experimental verifications. Neutron-scattering experiments could clarify the presence and the size of gaps in the dispersion. Low-temperature investigations of the structure would help to improve our understanding of the charge-ordered state. Low-temperature x-ray absorption data are required to determine the hole density in the ladders. Raman studies as a function of Ca concentration and temperature could verify that the features explained here are indeed connected to the occurrence of the charge-ordered state. Then, the peak position offers a sensitive tool to determine the modulation wave vector Q_{CO} .

In conclusion, the modulation of the exchange coupling

in the charge-ordered state of $\text{Sr}_{14}\text{Cu}_{24}\text{O}_{41}$ can explain the peculiar Raman data. The induced gap redistributes a large part of the spectral weight, giving rise to a sharp Raman peak. A comparison with the 2D cuprates is not appropriate. Strong quantum fluctuations are still the most likely candidate to explain their very broad Raman line.

We thank E. Müller-Hartmann, G. Blumberg, A. Gozar, and M. Braden for helpful discussions and the DFG for financial support in SP 1073 and in SFB 608.

-
- [1] S. A. Carter *et al.*, Phys. Rev. Lett. **77**, 1378 (1996).
 - [2] M. Uehara *et al.*, J. Phys. Soc. Jpn. **65**, 2764 (1996).
 - [3] T. Nagata *et al.*, Phys. Rev. Lett. **81**, 1090 (1998).
 - [4] L. P. Regnault *et al.*, Phys. Rev. B **59**, 1055 (1999).
 - [5] M. Matsuda, T. Yoshihama, K. Kakurai, and G. Shirane, Phys. Rev. B **59**, 1060 (1999).
 - [6] T. Fukuda, J. Mizuki, and M. Matsuda, Phys. Rev. B **66**, 012104 (2002).
 - [7] M. Braden, private communication.
 - [8] U. Ammerahl *et al.*, Phys. Rev. B **62**, 8630 (2000).
 - [9] V. Kataev *et al.*, Phys. Rev. B **64**, 104422 (2001).
 - [10] N. Nücker *et al.*, Phys. Rev. B **62**, 14384 (2000).
 - [11] Y. Mizuno, T. Tohyama, and S. Maekawa, J. Phys. Soc. Jpn. **66**, 937 (1997).
 - [12] E. M. McCarron, M. A. Subramanian, J. C. Calabrese, and R. L. Harlow, Mat. Res. Bull. **23**, 1355 (1988).
 - [13] A. F. Jensen, V. Petříček, F. K. Larsen, and E. M. McCarron III, Acta Cryst. **B53**, 125 (1997).
 - [14] S. Sugai and M. Suzuki, phys. stat. sol. (b) **215**, 653 (1999).
 - [15] K. P. Schmidt, C. Knetter, and G. S. Uhrig, Europhys. Lett. **56**, 877 (2001).
 - [16] A. Gozar *et al.*, Phys. Rev. Lett. **87**, 197202 (2001).
 - [17] C. Knetter, G. S. Uhrig, Eur. Phys. J. B **13**, 209 (2000).
 - [18] M. Matsuda *et al.*, J. Appl. Phys. **87**, 6271 (2000).
 - [19] M. Matsuda *et al.*, Phys. Rev. B **62**, 8903 (2000).
 - [20] T. Nunner *et al.*, Phys. Rev. B **66**, 180404 (2002).
 - [21] S. Brehmer *et al.*, Phys. Rev. B **60**, 329 (1999).
 - [22] Neglecting the two-spin exchange terms along the diagonals, our notation $J_{\perp}, J_{\parallel}, J_{\text{cyc}}$ is given in terms of the other notation $J_{\perp}^{\text{p}}, J_{\parallel}^{\text{p}}, J_{\text{cyc}}^{\text{p}}$ using cyclic permutations by $J_{\parallel} = J_{\parallel}^{\text{p}} + \frac{1}{4}J_{\text{cyc}}^{\text{p}}, J_{\perp} = J_{\perp}^{\text{p}} + \frac{1}{2}J_{\text{cyc}}^{\text{p}}$, and $J_{\text{cyc}} = J_{\text{cyc}}^{\text{p}}$ [21].
 - [23] Fig. 1 shows the periodicity; the modulation *phases* of the couplings cannot be read off because (i) Cu sites in the chains and ladders are not in line; (ii) each ladder is influenced by the four chains close by which are shifted by different amounts; (iii) the important oxygens are not depicted. For details see Ref. [13].
 - [24] E. Müller-Hartmann and A. Reischl, Eur. Phys. J. B **28**, 173 (2002).
 - [25] C. Knetter, K. P. Schmidt, M. Grüninger, and G. S. Uhrig, Phys. Rev. Lett. **87**, 167204 (2001).
 - [26] K. P. Schmidt, C. Knetter, and G. S. Uhrig, Acta Phys. Pol. B **34**, 1481 (2003).
 - [27] *Phase Transitions and Critical Phenomena*, edited by C. Domb and J. L. Lebowitz (Academic Press, New York, 1989), Vol. 13.